Global Displacement Speeds of Methane/Air Measured in a Fan-Stirred Flame Speed Vessel

Sankaranarayanan Ravi and Eric L. Petersen
Texas A&M University
College Station, Texas, USA

1 Introduction

Methane is the primary constituent of natural gas, and hence its burning characteristics are of immense interest to gas turbine combustor designers. It has been recently recognized that the turbulent flame speed is not a mere perturbation of the laminar flame to external flow disturbances [1]. In fact, chemical kinetics influences or fuel effects are persistent even under highly turbulent conditions. These factors necessitate the compilation of a database of turbulent burning velocities for such candidate fuels through carefully conducted experiments. Of primal importance to gas turbine combustion processes are the propagation characteristics of the flame in the high-intensity turbulence regime which are critical in predicting unsteady flame dynamic processes such as flashback and blowout.

This paper presents results from the turbulent combustion experiments of premixed methane/air mixtures conducted using a new fan-stirred flame speed vessel and is organized as follows. First, a detailed description of the experimental apparatus is provided. The flow field characteristics inside the vessel with the fans operating are then summarized. The experimental procedure and the analysis technique are then explained in detail. Finally, the measured flame speeds are compared with the predictions of a widely used correlation so as to benchmark the facility.

2 Facility Description

Laminar flame speed experiments have been performed at the authors' laboratory in a high-pressure cylindrical flame speed vessel [2,3]. This aluminum vessel (Al 7075) has an internal diameter of 305 mm and an internal length of 355 mm. High-pressure experiments up to initial pressures of 15 atm can be performed without any pressure rise during the usable part of the experiment. Optical-quality quartz windows at the two ends of the vessel enable visual tracking of the expanding flame up to a maximum diameter of 127 mm under constant-pressure conditions. The spark-ignited flame is imaged using a z-type schlieren setup used in combination with a high-speed camera (Photron Fastcam SA 1.1). The temperature inside the vessel is monitored using a k-type thermocouple, and typical initial temperatures are 296 ± 3 K.

This vessel was recently modified to conduct turbulent flame speed measurements. Four fans were installed symmetrically around the central circumference of the vessel to generate turbulence during the experiment. The fans are radial impellers with three backward-curved blades which direct the flow towards the vessel wall. They are made of aluminum (Al 6061-T6) with an outer diameter of 76.2 mm and a blade pitch angle of 20°. The reader is directed to another publication by the authors for further details on the fans [4]. These fans are fitted on steel shafts (A2 tool steel) that are polished to an extremely fine surface finish. Shaft sealing is provided by means of PTFE lip seals. High-speed bearings for the shafts are stacked inside cartridge housings that are directly mounted onto the vessel. Each fan is turned by a 2.25 HP router motor whose rotational speeds can be varied between 8,000 and 24,000 rpm. The impeller shafts are connected to the motor shafts by means of flexible couplings which can compensate for minor shaft misalignments. Figure 1 shows the actual experimental apparatus along with the 3D computer model.

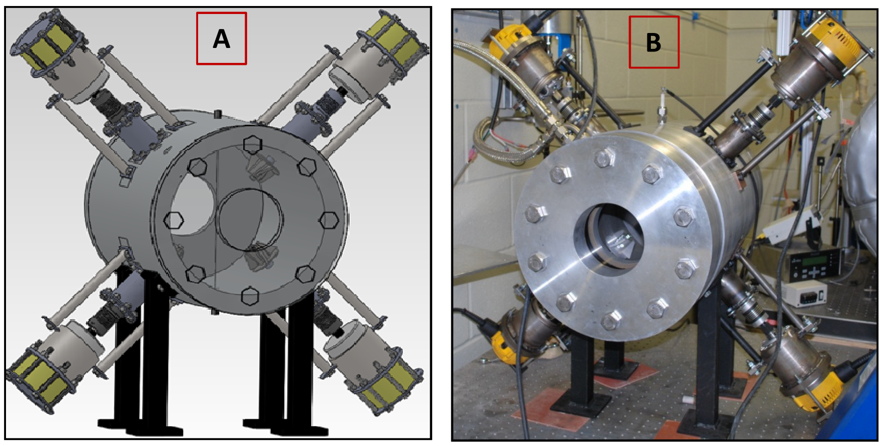

Figure 1. Fan-stirred flame speed vessel at Texas A&M. [A]: 3D rendering. [B]: Photograph of the facility.

3 Turbulence Statistics

Prior to modification of the laminar flame speed apparatus, a 1:1 scale acrylic model of the vessel was fabricated to characterize the generated turbulent field (using particle image velocimetry, or PIV). The details of this study are reported elsewhere [4], and so, only a brief summary of the important results is presented here. An average RMS turbulent intensity, $u' = 1.5$ m/s with negligible mean flow ($< 0.1\ u'$), was measured at the lowest fan speeds with an integral length scale (L) of 27mm. These values are used for this study. Additionally, the turbulent flow field exhibited two features: (1) homogeneity or spatial uniformity; and, (2) isotropy or directional equality of the velocity components in the two orthogonal directions at the center of the vessel. Both the homogeneity and isotropy ratios varied between 0.9 and 1.1 (ideal value being 1), thus providing stationary (no mean flow) and uniform perturbations (also called homogeneous and isotropic turbulence, HIT) during flame growth.

4 Experimental Procedure and Image Analysis

The turbulent combustion experiments follow the same procedure as the laminar flame speed experiments. First, the vacuum in the vessel is checked. Once a feasible vacuum is achieved, the gases are manometrically filled and allowed to mix in the vessel for a period of 30 minutes. All consumable gases for the experiments are of ultra-high purity grade. Prior to ignition, the fans are activated and the flow field inside the vessel is allowed to reach steady state turbulence, which takes as little as 10 seconds (as confirmed from PIV measurements). The mixture is then ignited, and the flame propagation event is recorded using the high-speed camera.

Sample images from a turbulent flame speed experiment are shown in Fig. 2. The schlieren images reveal lamella-like structures that constantly develop and wrinkle the flame surface as it grows in size.

The turbulent flame exhibits three-dimensionality indicative of varying propagation rates in different directions. This behavior is contrary to laminar flames where there is isotropic propagation which facilitates two-dimensional analysis of the flame with a near-circular projection [2,3].

Post processing is done using a MATLAB code that was developed in house [5]. The program tracks the flame boundary and estimates the area within the turbulent flame kernel for each frame, as shown in Fig. 2. The enclosed area is then used to compute the radius of a circle with an equivalent area. This is defined as the schlieren radius, r_{sch}.

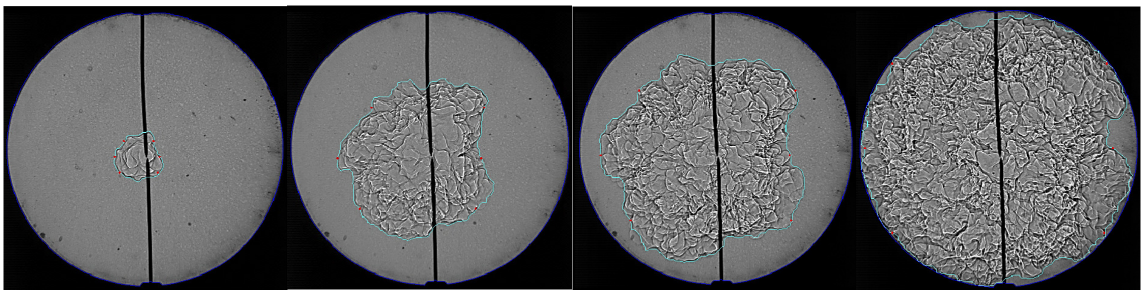

Figure 2.Turbulent flame propagation for methane/air at 1 atm, 298 K, φ=1.0, u′=1.5 m/s. The blue edge around the flame kernel is used to compute the enclosed area, from which the radius of the equivalent circle is estimated. The red points are from the six-point technique used for laminar flame speed experiments.

5 Flame Radius

Figure 3 shows the evolution of r_{sch} with time for stoichiometric methane in air at 1 atm, 298 K. Also included is the flame growth history of the same mixture for the laminar case. Whereas a perfectly linear slope that is indicative of constant flame speed (no flame acceleration) is seen for the laminar case, r_{sch} grows rapidly and nonlinearly for the turbulent case, suggesting varying turbulent flame speed with time. Also, the data density for the turbulent case was deliberately set to a higher value by adjusting the framing rate of the camera (15,000 for turbulent; 2,000 for laminar). This improvement in temporal resolution reduces errors in the time derivative estimates required for propagation rates (as is shown later).

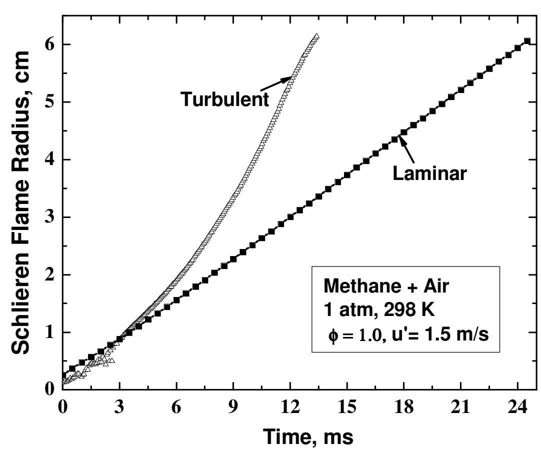

Figure 3. Flame radii evolutions of a laminar and a turbulent flame from the authors' laboratory. Acceleration of the flame for the latter case is evident.

6 Turbulent Propagation Rates

Unlike the laminar flame speed, a unified definition of turbulent propagation rate has not been established to facilitate comparison of data measured using different techniques. For example, the propagation rates obtained from a burner-type test facility are distinctly different from those of a fan-stirred flame bomb. This predicament is due to the fact that the measurement surfaces differ from technique to technique. The turbulent flame speed or the global displacement speed ($S_{T,0.1}$) is measured using schlieren imaging in a fan-stirred vessel, while the turbulent burning velocity ($S_{T,0.5}$) or the global consumption speed is estimated from a burner-type apparatus. The two definitions differ by the value of the reaction progress variable, $\langle \bar{c} \rangle$, on the surface used for measurement [6,7]. The leading edge of the schileren image represents an isothermal surface with a reaction progress variable value of $\langle \bar{c} \rangle \approx 0.1$. The turbulent burning velocity ($S_{T,0.5}$) obtained from Bunsen burner rigs correspond to a radius with $\langle \bar{c} \rangle \approx 0.5$, namely, $r_{0.5}$.

To determine the global displacement speed, the instantaneous turbulent flame speed, S_F, is first computed through Eq. (1) using a central difference technique. $S_{T,0.1}$ is then estimated by multiplying S_F with the density ratio of the burned to unburnt gases (continuity) following Eq. (2). Figure 4 shows the variation of the global displacement speed with the flame radius (and also time, but not shown) for two experimental runs of the same mixture. Also shown is the non-dimensional flame radius, $\bar{r}$, defined as the ratio of the schlieren flame radius to the integral length scale.

$$S_F = dr_{sch}/dt = (r_{sch}^{t+1} - r_{sch}^{t-1})/(2\Delta t) \tag{1}$$

$$S_{T,0.1} = (S_F)(\rho_b/\rho_u) \tag{2}$$

Despite the stochastic nature of the experiment, there is good agreement between the datasets. This repeatability is indicative of the fact that turbulent flame speed can be used as a meaningful quantity for defining the burning characteristics of fuels under turbulent conditions. Furthermore, $S_{T,0.1}$ increases with flame radius. This behavior is due to the wrinkling of the flame surface by eddies from the turbulent field. Wrinkling results in an increase in flame surface area which in turn causes an increase in burning velocity. Furthermore, only eddies smaller than the flame radius can affect the flame ball by penetrating into the reactive flame structure. Larger eddies have a mere kinematic effect on the flame kernel, thereby convecting it. Thus the flame is subjected to an increasing spectrum of eddies as it grows, which explains the increase in S_T with radius. $S_{T,0.1}$ at different values of $\bar{r}$ can be obtained from the line of best fit. One such linear fit and its statistical goodness of fit, r^2, are shown in Fig. 4. Typically, $S_{T,0.1}$ at $\bar{r}$ = 1-1.5 is quoted as the turbulent flame speed. For this range of $\bar{r}$, the flame is large enough that it would measure at least twice the integral length scale, and is also devoid of any residual effects from the ignition spark [6-8]. All measurements reported herein were taken at $\bar{r}$ = 1.

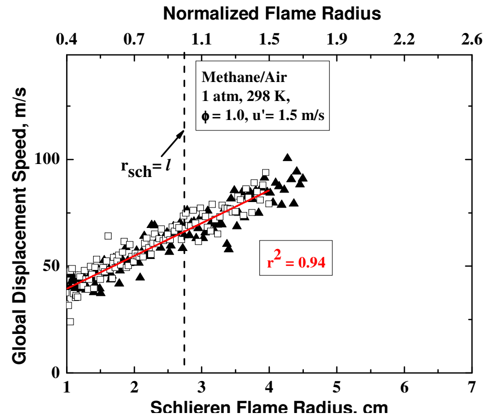

Figure 4. Global displacement speeds ($S_{T,0.1}$) at different flame radii. $S_{T,0.1}$ increases with flame size. Also shown is the non-dimensional radius, . The red line represents the line of best fit for the measured $S_{T,0.1}$ (symbols). The vertical dashed line denotes = 1 (when $r_{sch}= l$). Symbols represent two different experiments (solid triangles and open squares).

Figure 5 shows the global displacement speeds of methane/air at different equivalence ratios. The corresponding laminar flame speeds are shown as well. As evident, turbulence has increased the flame speeds at all mixture strengths. These measurements were made in the high-intensity turbulence regime (u'/S_L: 4-10 for the present study) in which there is an enhancement of flame propagation rates by the superimposed turbulent field due to intensified mass and heat transfer rates effected by turbulent diffusion. Figure 6 shows the turbulent combustion regime diagram (Borghi diagram) for the conditions investigated herein. The ratios of the flame properties (laminar flame thickness and laminar flame speed) relative to the turbulent parameters (RMS intensity and integral length scale) place them in the thin reaction zone. In this regime, the smallest eddies in the flow (Kolmogorov scale) can penetrate into the preheat zone of the flame and increase scalar mixing.

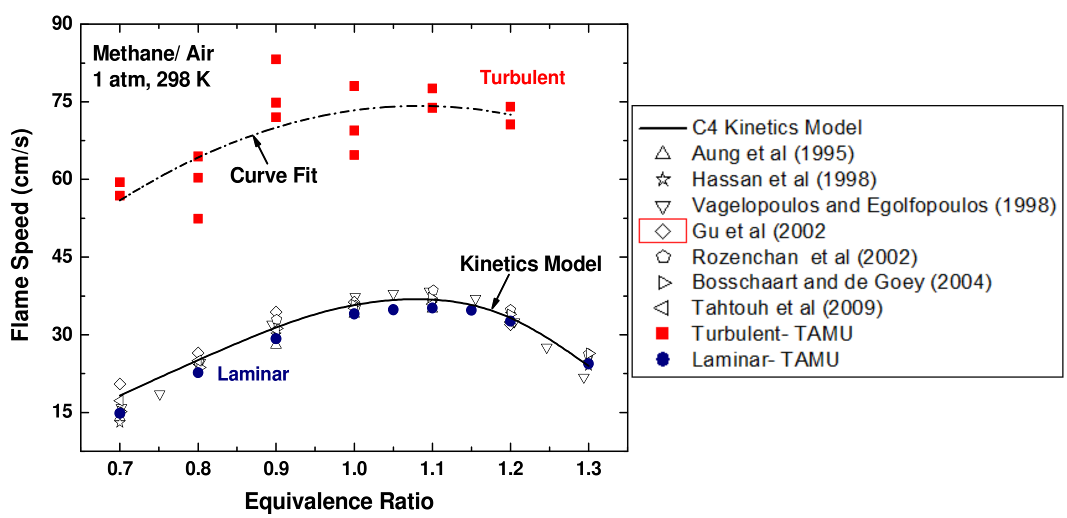

Figure 5. Global displacement speeds/ turbulent flame speeds ($S_{T,0.1}$) for methane/air at 1 atm, 298 K and u′= 1.5 m/s. Also shown are the laminar flame speeds (measurement and kinetics model predictions) at different equivalence ratios [3]. The measured laminar flame speeds agree well with those reported in the literature.

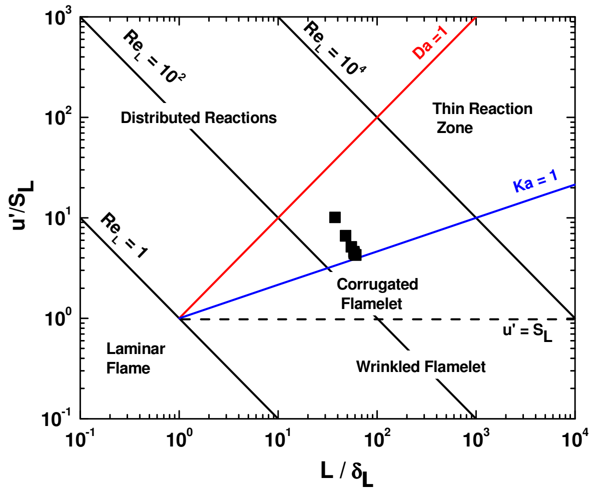

Figure 6. Turbulent combustion regime diagram (Borghi diagram). The conditions investigated herein are shown as symbols.

7 Data Validation

The measurements were validated by comparing with the data obtained from other facilities [8-10]. To facilitate comparison between different rig types, such as Bunsen burner and spherical bombs, $S_{T,0.5}$ was considered more feasible. The displacement speeds from this study were converted to turbulent burning velocities using the relation [8] shown in Eq. (3). First, the turbulent burning velocities were normalized by their corresponding laminar flame speeds. These normalized rates are plotted as a function of the product of the normalized intensity (u'/S_L) and pressure (p/p_0) (where, p is the test pressure and p_0 = 1 atm is the baseline pressure), as shown in Fig. 7. The propagation rates obtained from this study are consistent with a widely used correlation [10] developed from a database of turbulent burning velocities of methane [9]. While a more-rigorous comparison is proposed for future work, the current close agreement is encouraging and serves as a good validation tool for the newly developed facility.

$$S_{T,0.5}/S_{T,0.1} = (r_{0.5}/r_{sch})^2 = (1.4)^2 = 1.9 \quad (3)$$

8 Conclusion

This study presented a new fan-stirred facility that can be used to measure the turbulent flame speeds of different fuels. The current setup allowed for measurement of the global displacement speeds. Turbulent combustion experiments of premixed methane/air over a wide range of equivalence ratios (0.7-1.2) were conducted. The resulting data showed good repeatability as well as agreement with those measured in other facilities. Future work includes extension of these results to different turbulent conditions (u′ and *l* variations).

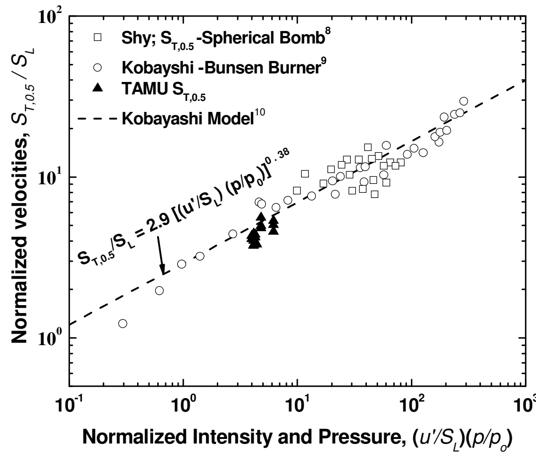

Figure 7. Turbulent burning velocities of methane/air at different conditions. The result from the present study agrees well with the data from other facilities [8,9] as well as with the turbulent combustion model (dashed line) [10]. The displacement speeds from the present study are converted to burning velocities using the same procedure outlined in [8].

References

[1] Lipatnikov AN, Chomiak J. (2002). Turbulent Flame Speed and Thickness: Phenomenology, Evaluation, and Application in Multi-Dimensional Simulations. Prog. Energ. Combust. 28:1.

[2] de Vries J. (2009). A Study on Spherical Expanding Flame Speeds of Methane, Ethane and Methane/ethane Mixtures at Elevated Pressures. PhD Dissertation, Texas A&M University, USA.

[3] Lowry W et al. (2011). Laminar Flame Speed Measurements and Modeling of Pure Alkanes and Alkane Blends at Elevated Pressures. J Eng. Gas Turb. Power. 133: 091501-1.

[4] Ravi S, Peltier SJ, Petersen EL. (2013). Analysis of the Impact of Impeller Geometry on the Turbulence Statistics Inside a Fan-stirred, Cylindrical Flame Speed Vessel using PIV. Exp. Fluids. 54:1424.

[5] Krejci MC et al. Laminar Flame Speed and Ignition Delay Time Data for the Kinetic Modeling of Hydrogen and Syngas Fuel Blends. J Eng. Gas Turb. Power. (accepted for publication); also, ASME Paper GT2012-69290.

[6] Bradley D, Lawes M, Mansour MS. (2011). Correlation of Turbulent Burning Velocities of Ethanol-Air, Measured in a Fan-Stirred Bomb up to 1.2 MPa. Combust. Flame. 158: 123.

[7] Mandilas C et al. (2007). Effects of Hydrogen Addition on Laminar and Turbulent Premixed Methane and Iso-Octane-Air Flames. Proc. Combust. Inst. 21:1443.

[8] Liu CC et al. (2012). High-Pressure Burning Velocities Measurements for Centrally-Ignited Premixed Methane/Air Flames Interacting with Intense Near-Isotropic Turbulence at Constant Reynolds Numbers. Combust. Flame. 159:2608.

[9] Kobayashi H et al. (1996). Burning Velocity of Turbulent Premixed Flames in a High-Pressure Environment. Proc. Combust. Inst. 26: 389.

[10] Kobayashi H, Kawabata Y, Maruta K. (1998). Experimental Study on General Correlation of Turbulent Burning Velocity at High Pressure. Proc. Combust. Inst. 27: 941.